Letter to the Editor:
Can Body-Worn Devices be used for Measuring Personal Exposure to mm Waves?

Arno Thielens*, Luc Martens *, and Wout Joseph *

*Department of Information Technology, Ghent University, Ghent, Belgium

Corresponding author: Arno Thielens, Ghent University, Technologiepark 15, B-9052 Ghent, Belgium, email: arno.thielens@intec.ugent.be, phone: +32 9 33 14918, fax: +32 9 33 14899

Running title: On-Body Measurements of mm-Waves

Grant sponsor info: Arno Thielens is a post-doctoral fellow of Flanders Innovation and Entrepreneurship under agreement no. 150752.

Conflict of interest: none

Abstract- 5th generation (5G) telecommunication networks will require more bandwidth and will use mm-waves (30-300 GHz). Consequently, the aperture of the antennas that are used for electromagnetic field measurements will be reduced in comparison to the ones currently used for lower frequencies (0.1 – 6 GHz). In combination with existing limits on the incident power density, prescribed by exposure guidelines, this provides an upper limit to received powers during exposure measurements. Simultaneously, an increase in the noise floor of the transmitted signals will occur. These effects limit the dynamic range of the measurements to 53 dB (2 x 10^5) at 300 GHz and 73 dB (2 x 10^7) at 30 GHz, which are determined using a simplified model. Additional propagation losses that exceed this dynamic range can occur during on-body measurements. Therefore, in future wireless networks, an on-body measurement of the incident power density cannot be guaranteed using a single antenna. This effect is problematic for both occupational measurements and epidemiological studies. We propose to use multiple, dynamic antennas on the body instead.

Keywords- mm-waves; 5th generation networks; body path loss; broadband telecommunication; thermal noise

5G networks will cause personal exposure electromagnetic fields (EMFs) in the mm-wave range. This exposure can be caused by one's own use of a mm-wave device or by the network and other users during communication, beam-alignment, or physical channel control [Shokri-Ghadikolaei et al., 2015]. A common approach to measure personal exposure to EMFs is the use of personal exposimeters [Bolte et al., 2011]. These are body-worn device that contain an antenna, which records the EMFs on the body. Several studies have already shown that these devices underestimate EMFs due to shielding of the body [Neubauer et al., 2010; Bolte et al., 2011; Thielens et al., 2016].

It is expected that the effect of body shielding on the detection of EMFs could become even more critical in the mm-wave region due to three effects. First, the aperture of body-worn antennas is of the order of the wavelength squared [Balanis, 1982]. A smaller antenna aperture implies that a smaller power will be received on an antenna exposed to a constant incident power density. Usually this is compensated by using active, high-gain arrays of antennas [Pi et al., 2011; Thors et al., 2016; Zhao et al., 2016] and applying dynamic beam-steering and -scanning [Zhao et al., 2016]. However, this technique is not applied in exposure measurements, since the measurement device is not controlled by the network. The best option in exposure measurements is to use an (array of) antenna(s) with an isotropic radiation pattern. Both radial and axial anisotropy of an exposimeter cannot be compensated using calibration of the device [Bolte et al., 2011; Thielens et al., 2016] and will lead to an unwanted over or underestimation of the exposure. Second, the broad bandwidth of 5G telecommunications is associated with a relatively high thermal noise floor [Pi et al., 2015]. It should be clear that the combination of a low received power on the antenna and a high noise floor is not optimal for exposure measurements. As a third factor, the limits on the incident power density are constant in the mm-wave band [FCC, 1997; ICNIRP, 1998; IEEE, 2005].

Consequently, this paper investigates the plausibility of on-body measurement of personal exposure to mm-waves. To this aim, an on-body propagation model [Mavridis et al., 2014] that uses a simplified human body, exposed to plane waves at 30-300 GHz is considered to estimate the shadowing caused by the human body. The novelties of this study are that, for the first time, the dynamic range of on-body personal exposure measurements in the mm-wave range is estimated and that it is demonstrated that single on-body nodes cannot guarantee reliable personal exposure measurements of mm waves in all potential exposure conditions.

A body-worn receiving antenna (RX) is used to register the incident power density (S_{inc}) in the mm-wave range during personal exposure measurements. The received power on the RX (P_r) is related to S_{inc} through the antenna aperture (AA) of the on-body antenna: $P_r = AA \times S_{inc}$. The AA depends heavily on the design and type of the used antenna. In order to use a single (on-body) antenna as an accurate measurement device for S_{inc}, the antenna must be isotropic. A dependency of the AA on the angles of incidence would introduce a dependency of P_r on the angles of incidence, which (for a single antenna) cannot be compensated if the angles of incidence are unknown [Thielens et al., 2016]. The AA of an isotropic antenna is equal to the wavelength squared λ^2 divided by 4π [Balanis, 1982]. The incident EMFs sometimes have to propagate around/on the body in order to reach the RX. This is accompanied with an on-body path loss (BPL) that will reduce P_r. In order to receive power on the body, the BPL should be low enough. The incident EMFs can be partly absorbed in the human body. Therefore, several standardization organizations have issued limits on S_{inc} [FCC, 1997; ICNIRP, 1998; IEEE, 2005]. The spatially averaged limits for the general public in the mm-wave range are 10 W/m² averaged over 20 cm² from 30-300 GHz [ICNIRP, 1998] 10 W/m² averaged over 100 cm² from 30 – 100 GHz [IEEE, 2005], and (90 x f – 7000)/200 W/m² (with f the frequency in GHz) from

100 – 300 GHz. Additionally, the ICNIRP [1998] defines a 1 cm² averaged limit of 200 W/m² from 30 - 300 GHz. Spatial peak values are limited to 200 W/m² [IEEE, 2005] and 10 W/m² from 30 – 100 GHz [FCC, 1997].

Any device in thermal equilibrium that uses charges to register signals is confronted with thermal noise. This thermal noise, which in this case manifests itself as received noise power on the antenna (N, measured in dBW), increases proportional to the logarithm of the used bandwidth (BW) [Balanis, 1982]:

$$N(dBW) = 10 \times \ log_{10}(k_B \times T \times \Delta f) \quad (1)$$

with T the temperature in K, k_B = 1.38 x 10^{-23} J/K Boltzmann's constant, and Δf the BW in Hz. The existing standards for telecommunication at mm waves (mainly around 60 GHz) assume BWs > 1 GHz [IEEE, 2009, 2012]. A BW higher than 1 GHz corresponds to a noise floor higher than -114 dBW (4 x 10^{-12} W) at T = 290 K, see Eq. 1. A lower physical temperature (T) would yield less noise. However, we assume a minimal T of 290 K at distances of a few mm from the human body. Given the maximal S_{inc} of 10 W/m², the maximal received power for an ideal isotropic antenna will range from -61 dBW (8 x10^{-7} W) at 300 GHz to -41 dBW (8 x 10^{-5} W) at 30 GHz. The noise floor of -114 dBW (4 x 10^{-12} W) implies small dynamic ranges for the received power of 73 dB (2 x 10^{7}) at 30 GHz, 67 dB (5 x 10^{6}) at 60 GHz, and 53 dB (2 x 10^{5}) at 300 GHz. The BPL cannot exceed these values in order to receive a signal on a body-worn device.

In order to quantify the BPL induced due to shielding of the human body, we have worked with the model proposed in Mavridis et al. [2014]. Figure 1 illustrates the studied model and exposure scenario. This model has disadvantages: it models the human body as a cylinder, see Fig. 1, which is not realistic, it models the skin as a perfect electrical conductor (PEC), and it models the exposure as a plane wave, which can be a narrow beam in reality. However, it has the advantage that it proposes a closed analytical expression for the BPL around a cylinder at mm waves, which is experimentally validated at 60 GHz for Transverse-Magnetic (TM)-polarized waves. The model underestimates the BPL for Transverse-Electric (TE)-polarized plane waves at 60 GHz [Mavridis et al., 2014]. In the lit zone of the body the BPL is close to 0 dB and can even be lower due to reflections [Mavridis et al., 2014]. The fields in the region that is shielded by the body are attenuated and are determined using the model of Mavridis et al. [2014], see Fig. 1, as a function of the azimuth angle (ϕ) and the radial distance (ρ) from a cylinder with radius (r).

Figure 2 shows the BPL at 60 GHz (a potential 5G communication frequency [Rappaport et al., 2013]) as function of ϕ in the zone shielded by the cylinder, where $\phi = 0°$ corresponds to the direction of incidence of the plane wave. A separation of 5 mm is chosen since this corresponds to $\lambda/2$ for the highest λ the mm-wave region. We assume that a minimal separation distance to the body of $\lambda/2$ is necessary for proper antenna operation. We have chosen to show results for radii of 0.1 m and 0.25 m, since these correspond to the range of radii of the standardized spheroids that are used to model the human body in Durney et al. [1986] (e.g., an adult human is modelled by a spheroid with r = 0.138 m). The BPL is close to zero at the edge of the shielded zone, but increases exponentially as a function of ϕ. Figure 3 shows the BPL at 5 mm from the cylinder and the worst-case angle $\phi = 180°$ as a function of frequency (30-300 GHz). The BPL increases with both r and with frequency. Figure 2 shows estimated BPL values at 60 GHz that clearly exceed the 67 dB (5 x 10^6) dynamic range, which is available at 60 GHz without body shielding. This implies that it is impossible to measure S_{inc} in a large part (78° at 5 mm from a cylinder with r = 0.25 m) of the shielded zone of the body at 60 GHz. This effect is problematic for both occupational measurements and epidemiological studies. Figure 3 shows that this problem occurs at all mm-wave frequencies. Even if 5G would require less BW than 1 GHz, we would still expect problems in the mm-wave region. A BW of 50 kHz (BW used for

PHY CC at mm waves [Shokri-Ghadikolaei et al., 2015]) would have a 43 dB (2 x 10^4) reduced noise floor, which is still too high for f > 100 GHz, see Figure 3.

The values of the BPL have to be validated, but the measurements performed in Mavridis et al. [2014] suggest that a similar BPL will be found on real human bodies. In Mavridis et al. [2015], the PL between an off-body TX and an RX close (< 30 cm) to the body at 60 GHz was measured. BPL values higher than 80 dB (10^8) were found at the back of the body. In Petrillo et al. [2014], the BPL was measured on the chest of a human subject at 60 GHz. The BPL was found to increase with TX-RX separation on the body and reached values up to 80 dB (10^8). Gustafson et al. [201] found lower BPL values at 60 GHz, up to 52 dB (1.6 x 10^5), but only considered smaller shadowing parts of the human body such as the legs, the shoulders, and the neck or placed the RX at larger distances (70 cm) from the subject. Chahat et al. [2013] predicted and measured losses > 60 dB (10^6) after 0.25 m of propagation for a dipole placed at the surface of a flat phantom at 60 GHz.

We propose two solutions to this problem. A first solution is the deployment of multiple on-body antennas on different locations of the human body in such a way that one of them is always lit (no significant BPL). This solution has already been proposed in Bolte et al. [2011] and Thielens et al. [2016] and has shown to lead to an improved assessment of S_{inc} for lower frequencies (0.1 – 6 GHz). This paper shows that in the mm-wave region the use of multiple on-body antennas might not only be beneficial, but necessary. A second approach is the use of multiple, dynamic, directional antenna(s) (arrays) [Shokri-Ghadikolaei et al., 2015] that can apply network-independent beam-steering and beam-scanning in order to counter BPL by increasing their gain in the direction of incidence. The beam-control has to be independent of the telecommunication networks, since otherwise exposure from multiple networks and users might be missed. This last method has disadvantages: applying beam-steering will take more time than it takes for the exposure to occur and some instances of exposure might be missed due to deafness of the antennas [Shokri-Ghadikolaei et al., 2015].

To conclude, the feasibility of measurements of the incident power density of mm-waves (30 - 300 GHz) using single on-body antennas is investigated. The incident power density is limited by guidelines (10 W/m^2) and has to be received by antennas with a relatively small antenna aperture (< 8 mm^2). This poses an upper limit to the potentially received power on the human body (< 80 μW). The received power on an on-body antenna can be lower due to propagation losses on the body. However, the received power may not be lower than the noise floor, which is expected to increase to values higher than -114 dBW (4 x 10^{-12} W) due to an increasing bandwidth. An on-body propagation model for incident mm-waves shows that the body can block all potential mm-wave signals at the envisioned bandwidth, when it is located in between the incident plane wave and the receiver. This indicates that single on-body antennas cannot be used for measurements of exposure to mm-waves. A potential solution is the use of multiple, dynamic antennas or arrays placed on the human body.

REFERENCES

Balanis CA. 1982. Antenna Theory: Analysis and Design. Hoboken, New Jersey: John Wiley & Sons.

Bolte JFB, Van der Zande G, Kamer J. 2011. Calibration and uncertainties in personal exposure measurements of radiofrequency electromagnetic fields. Bioelectromagnetics 32:652–663.

Chahat N, Valerio G, Zhadobov M, Sauleau R. 2013. On-Body Propagation at 60 GHz. IEEE TAP 61(4):1876-1887.

Durney CH, Massoudi H, Iskander MF. 1986. Radiofrequency Radiation Dosimetry Handbook. Report USAFSAM-TR- 85-73. Brooks Air Force Base, TX: United States Air Force School of Aerospace Medicine.

Federal Communications Commission (FCC). 1997. Code of Federal Regulations CFR title 47, part 1.1310, Radiofrequency radiation exposure limits.

Gustafson C, Tuvesson F. 2012. Characterization of 60 GHz Shadowing by Human Bodies and Simple Phantoms. Radioengineering 21(4):979-984.

IEEE International Committee on Electromagnetic Safety Std. 2005. C95.1-2005 Safety Levels with Respect to Human Exposure to Radio Frequency Electromagnetic Fields, 3 KHz to 300 GHz.

IEEE. 802.15.3c. 2009. Standard for Information Technology-Telecommunications and Information Exchange between systems-Local and Metropolitan networks-Specific requirements-Part 15.3: Wireless Medium Access Control (MAC) and Physical Layer (PHY) Specifications for High Rate Wireless Personal Area Networks (WPANs) amendment 2: Millimeter-wave based Alternative Physical Layer Extension.

IEEE. 802.11ad. 2012. IEEE Standard for Information technology--Telecommunications and information exchange between systems--Local and metropolitan area networks--Specific requirements-Part 11: Wireless LAN Medium Access Control (MAC) and Physical Layer (PHY) Specifications Amendment 3: Enhancements for Very High Throughput in the 60 GHz Band.

ICNIRP. 1998. Guidelines for limiting exposure to time-varying electric, magnetic, and electromagnetic fields (up to 300 GHz). Health Phys 74:494–522.

Mavridis T, Petrillo L, Sarrazin J, Lautru D, Benlabri-Delaï A, De Doncker P. 2014. Theoretical and Experimental Investigation of a 60-GHz Off-Body Propagation Model. IEEE TAP 62(1):393-402.

Mavridis T, Petrillo L, Sarrazin J, Benlabri-Delaï A, De Doncker P. 2015. Near-Body Shadowing Analysis at 60 GHz. IEEE TAP 63:4505-4511.

Neubauer G, Cecil S, Giczi W, Petric B, Preiner P, Fröhlich J, Röösli M. 2010. The association between exposure determined by radiofrequency personal exposimeters and human exposure: A simulation study. Bioelectromagnetics 31:535–545.

Petrillo L, Mavridis T, Sarrazin J, Benlarbi-Delaï A, De Doncker P. 2014. Statistical On-Body Measurement Results at 60 GHz. IEEE TAP 63(1):400-403.

Pi A, Khan F. 2011. An introduction to millimeter-wave mobile broadband systems. IEEE Comm Mag 49(6):101–107.

Rappaport TS, Sun S, Mayzus R, Zhao H, Azar Y, Wang K, Wong GN, Schulz JK, Samimi M, Gutierrez F. 2013. Millimeter Wave Mobile Communications for 5G Cellular: It Will Work! IEEE Access 1:335–349.

Shokri-Ghadikolaei H, Fischione C, Fodor G, Popovski P, Zorzi M. 2015. Millimeter Wave Cellular Networks: A MAC Layer Perspective. IEEE Trans on Comm 63(10):3437–3458.

Thielens A, Vanveerdeghem P, Van Torre P, Gängler S, Roosli M, Rogier H, Martens L, Joseph W. 2016. A Personal, Distributed Exposimeter: Procedure for Design, Calibration, Validation, and Application. Sensors 16(2): 180.

Thors B, Colombi D, Ying Z, Bolin T, Tornevik C. 2016. Exposure to RF EMF from Array Antennas in 5G Mobile Communication Equipment. IEEE Access 4:7469-7478.

Zhao K, Ying Z, He S. 2016. EMF Exposure Study Concerning mmWave Phased Array in Mobile Devices for 5G Communication. IEEE AWPL 15:1132-1135.

Figure Captions

Fig. 1. Configuration of the exposure scenario used to model BPL.

Fig. 2. 60 GHz BPL at 5 mm from the surface of the cylinder as a function of the azimuth angle ϕ, for radii of 0.1 m and 0.25 m. BPL for a TM-polarized incident wave is shown in black, while BPL for a TE-polarized incident wave is shown in grey. The angle of incidence $\phi = 0°$.

Fig. 3. BPL at azimuth angle $\phi = 180°$ as a function of the frequency of the incident wave for radii r of 0.1 m and 0.25 m. BPL for a TM-polarized incident wave is shown in black, while BPL for a TE-polarized incident wave is shown in grey. The angle of incidence $\phi = 0°$.

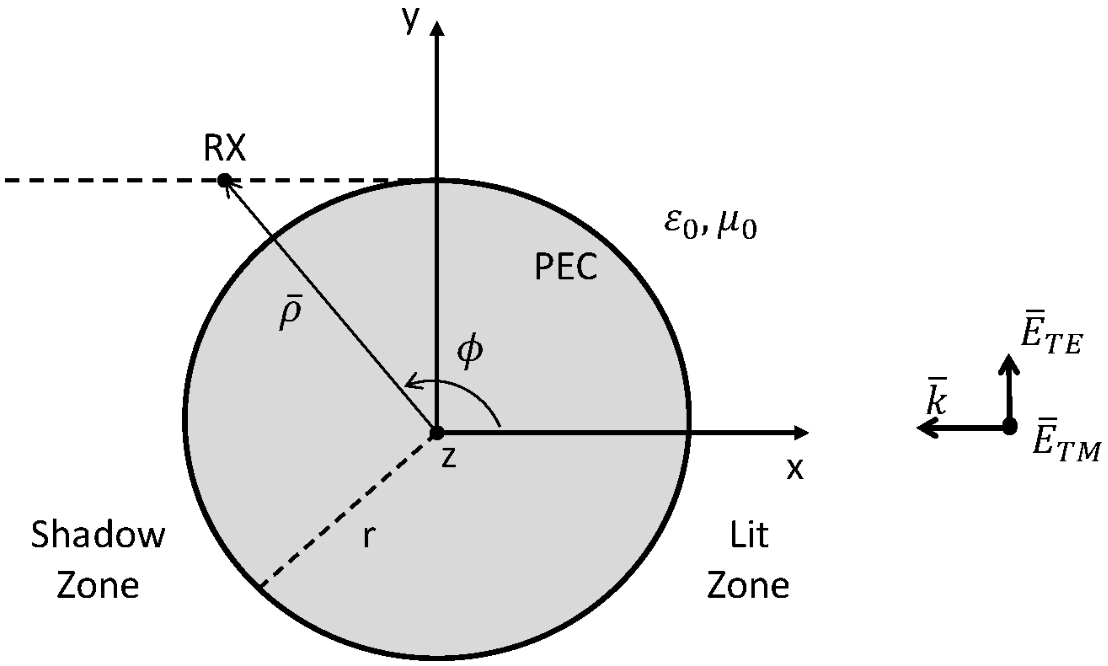

y
RX
ε_0, μ_0
PEC
$\bar{\rho}$
ϕ
$\bar{E}_{TE}$
$\bar{k}$
$\bar{E}_{TM}$
z
x
Shadow Zone
r
Lit Zone

Figure 1

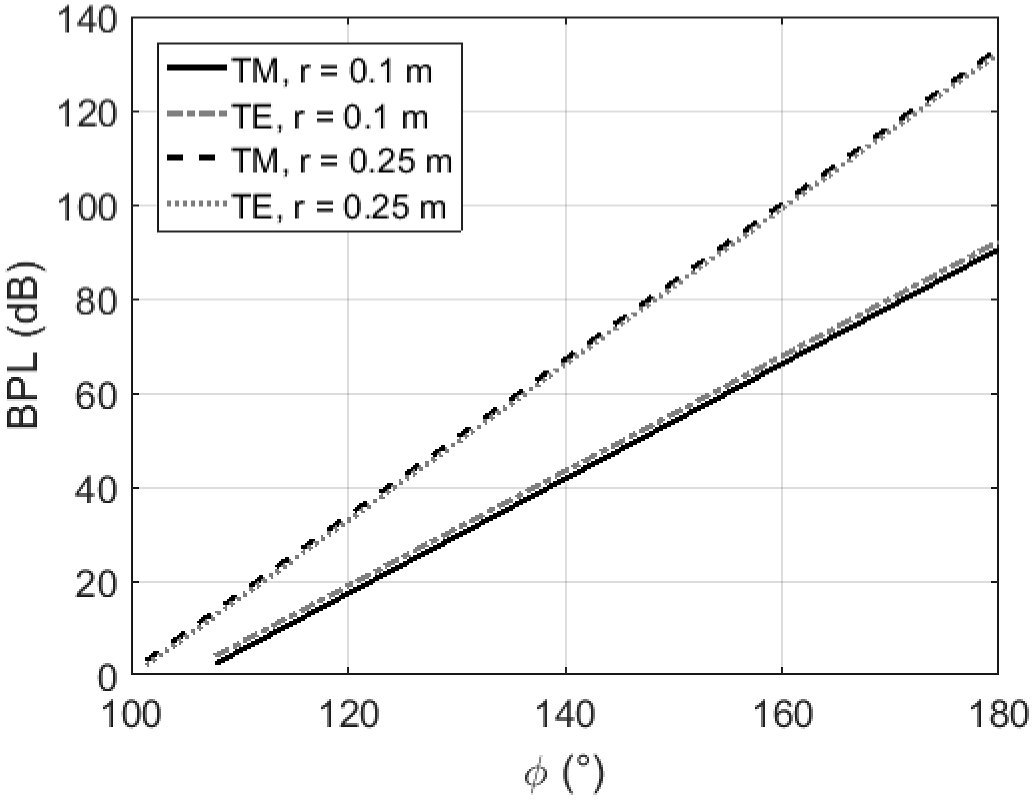

TM, r = 0.1 m
TE, r = 0.1 m
TM, r = 0.25 m
TE, r = 0.25 m
BPL (dB)
0
20
40
60
80
100
120
140
100
120
140
160
180
ϕ (°)

Figure 2

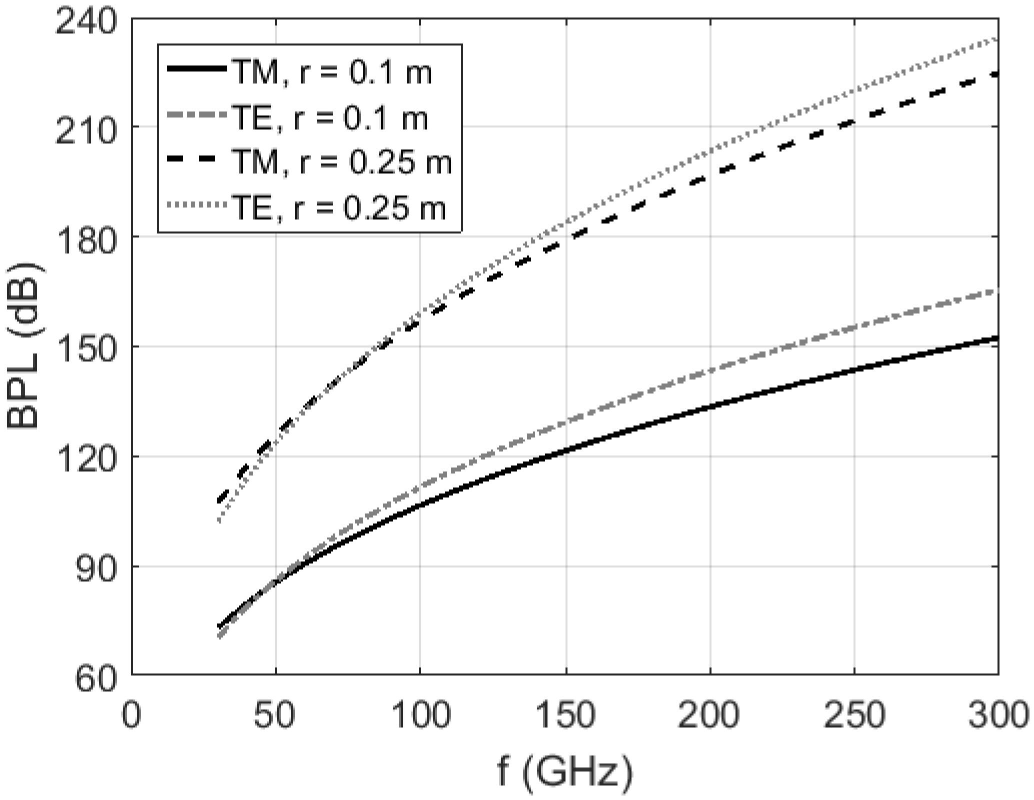
240
210
180
150
120
90
60
BPL (dB)
0
50
100
150
200
250
300
f (GHz)
TM, r = 0.1 m
TE, r = 0.1 m
TM, r = 0.25 m
TE, r = 0.25 m

Figure 3